Inorganic Chemistry
Article

Inorg. Chem. **2010**, *49*, 11525–11531 **11525**
DOI: 10.1021/ic101628z

Diruthenium Compounds Bearing Equatorial Fc-containing Ligands: Synthesis and Electronic Structure

Darryl A. Boyd,[†] Zhi Cao,[†] You Song,[‡] Tian-Wei Wang,[‡] Phillip E. Fanwick,[†] Robert J. Crutchley,[§] and Tong Ren*,[†]

[†]*Department of Chemistry, Purdue University, 560 Oval Drive, West Lafayette, Indiana 47907, United States,*
[‡]*School of Chemistry and Chemical Engineering, Nanjing University, Nanjing 210093, China, and*
[§]*Department of Chemistry, Carleton University, Ottawa ON K1S 5B6, Canada*

Received August 10, 2010

Previously, the synthesis of compounds $Ru_2(D(3,5\text{-}Cl_2Ph)F)_{4-n}(O_2CFc)_nCl$ (n = 1, **3a**; 2, **4a**), where D(3,5-Cl_2Ph)F is *N*,*N*′-di(3,5-dichlorophenyl)formamidinate, from the carboxylate exchange reactions between $Ru_2(D(3,5\text{-}Cl_2Ph)F)_{4-n}(OAc)_nCl$ and ferrocene carboxylic acid was communicated. Reported herein is the preparation of analogous compounds $Ru_2(DmAniF)_{4-n}(O_2CFc)_nCl$ (n = 1, **3b**; 2, **4b**), where DmAniF is *N*,*N*′-di(3-methoxyphenyl)formamidinate, from $Ru_2(DmAniF)_{4-n}(OAc)_nCl$. Compounds **3** and **4** were characterized with various techniques including X-ray structural determinations of **3a** and **4a**. Voltammetric behaviors of compounds **3** and **4** were investigated, and stepwise one-electron ferrocene oxidations were observed for both compounds **4a** and **4b**. Spectral analysis of the monocations $[\mathbf{4}]^+$ indicated that they are the Robin−Day class II mixed valent $[Fc\cdots Fc]^+$ species. Measurement and fitting of magnetic data (χT) of **4a** between 2 and 300 K revealed a typical zero-field splitting of a S = 3/2 center with D = 77 cm^{-1}, while those of $[\mathbf{4a}]BF_4$ are consistent with the presence of S = 3/2 (Ru_2) and S = 1/2 (Fc^+) centers that are weakly coupled ($zJ = -0.76$ cm^{-1}).

Introduction

Electron transfer (ET) is paramount to both chemical and life sciences, and recent pushes in research areas such as artificial photosynthesis and photovoltaics provide new impetus for the understanding and control of ET processes. Intramolecular ET within the supramolecular assemblies of dinuclear and polynuclear paddlewheel species has been explored by many groups, and representative studies include those based on Mo_2/W_2 building blocks[1,2] and extended metal-chain compounds.[3] Work conducted in the former area focuses on the ET mediated by the bridging ligand, typically a dicarboxylate, at equatorial positions, and the facile ET (class III mixed valency) observed in these systems is attributed to efficient mixing between the δ(MM) and π(carboxylate) orbitals.[2] On the other hand, highly efficient charge transfer along the axial direction either between two Ru_2 units or across one Ru_2 unit has been demonstrated by us and Lehn et al.,[4−7] where the mixing between π^*(Ru−Ru) and π(C≡C) orbitals holds the key.[7] Obviously, we have been curious about the ET processes along the equatorial direction of the Ru_2 coordination sphere. The initial effort was based on a dimer of Ru_2 units linked by the homocoupled *N*,*N*′-dimethyl-4-ethyne-benzamidinate ligand, where the ET between two Ru_2 centers separated by *ca.* 20 Å was deemed negligible on the basis of voltammetric studies.[8] More recently, we started to probe the equatorial ET within the Ru_2 coordination sphere by using ferrocene carboxylate ligands.[9]

*To whom correspondence should be addressed. E-mail: tren@purdue.edu.

(1) Cotton, F. A.; Lin, C.; Murillo, C. A. *Acc. Chem. Res.* **2001**, *34*, 759. Cotton, F. A.; Lin, C.; Murillo, C. A. *Proc. Natl. Acad. Sci. U.S.A.* **2002**, *99*, 4810. Cotton, F. A.; Donahue, J. P.; Murillo, C. A. *J. Am. Chem. Soc.* **2003**, *125*, 5436. Chisholm, M. H. *Struct. Bonding* (*Berlin*) **2010**, *136*, 29. Bursten, B. E.; Chisholm, M. H.; Clark, R. J. H.; Firth, S.; Hadad, C. M.; Wilson, P. J.; Woodward, P. M.; Zaleski, J. M. *J. Am. Chem. Soc.* **2002**, *124*, 12244. Bursten, B. E.; Chisholm, M. H.; Clark, R. J. H.; Firth, S.; Hadad, C. M.; MacIntosh, A. M.; Wilson, P. J.; Woodward, P. M.; Zaleski, J. M. *J. Am. Chem. Soc.* **2002**, *124*, 3050. Han, M. J.; Liu, C. Y.; Tian, P. F. *Inorg. Chem.* **2009**, *48*, 6347.
(2) Chisholm, M. H.; Patmore, N. J. *Acc. Chem. Res.* **2007**, *40*, 19. Chisholm, M. H.; Macintosh, A. M. *Chem. Rev.* **2005**, *105*, 2949.
(3) Liu, I. P. C.; Wang, W. Z.; Peng, S. M. *Chem. Commun.* **2009**, 4323. Berry, J. F. *Struct. Bonding* (*Berlin*) **2010**, *136*, 1. Yin, C. X.; Huang, G. C.; Kuo, C. K.; Fu, M. D.; Lu, H. C.; Ke, J. H.; Shih, K. N.; Huang, Y. L.; Lee, G. H.; Yeh, C. Y.; Chen, C. H.; Peng, S. M. *J. Am. Chem. Soc.* **2008**, *130*, 10090. Chen, I. W. P.; Fu, M. D.; Tseng, W. H.; Yu, J. Y.; Wu, S. H.; Ku, C. J.; Chen, C. H.; Peng, S. M. *Angew. Chem., Int. Ed.* **2006**, *45*, 5814.
(4) Ren, T. *Organometallics* **2005**, *24*, 4854.
(5) Ren, T.; Zou, G.; Alvarez, J. C. *Chem. Commun.* **2000**, 1197. Xu, G.-L.; Zou, G.; Ni, Y.-H.; DeRosa, M. C.; Crutchley, R. J.; Ren, T. *J. Am. Chem. Soc.* **2003**, *125*, 10057. Shi, Y.; Yee, G. T.; Wang, G.; Ren, T. *J. Am. Chem. Soc.* **2004**, *126*, 10552. Ying, J.-W.; Liu, I. P.-C.; Xi, B.; Song, Y.; Campana, C.; Zuo, J.-L.; Ren, T. *Angew. Chem., Int. Ed.* **2010**, *49*, 954. Wong, K.-T.; Lehn, J.-M.; Peng, S.-M.; Lee, G.-H. *Chem. Commun.* **2000**, 2259.
(6) Xu, G.-L.; DeRosa, M. C.; Crutchley, R. J.; Ren, T. *J. Am. Chem. Soc.* **2004**, *126*, 3728. Xi, B.; Xu, G. L.; Fanwick, P. E.; Ren, T. *Organometallics* **2009**, *28*, 2338.
(7) Xu, G.-L.; Crutchley, R. J.; DeRosa, M. C.; Pan, Q.-J.; Zhang, H.-X.; Wang, X.; Ren, T. *J. Am. Chem. Soc.* **2005**, *127*, 13354.
(8) Chen, W.-Z.; Ren, T. *Inorg. Chem.* **2006**, *45*, 9175.
(9) Boyd, D. A.; Crutchley, R. J.; Fanwick, P. E.; Ren, T. *Inorg. Chem.* **2010**, *49*, 1322.

Published on Web 11/11/2010

Since its discovery, ferrocene has been a staple in the area of electroanalytical chemistry.[10] The use of ferrocene as the probe for ET can be traced to the pioneering effort of Cowan et al.[11] Recent examples using ferrocene as the probe for intramolecular ET in inorganic species include those of mononuclear species,[12] clusters,[13] base-free porphyrins,[14] and dendrimers.[15] Trimetallic paddlewheel compounds, $M_3(dpa)_4(C{\equiv}CFc)_2$ with M = Co and Ru (dpa = 2,2′-dipyridylamide), were reported by Cotton et al.[16] and Peng et al.,[17] respectively, and weak electronic delocalization between two axial Fc units was inferred from voltammetric data in both cases. The *trans*-$Ru_2(DMBA)_4(C_{2n}Fc)_2$ type compounds developed in our laboratory exhibit much stronger couplings between two axial ferrocenyl groups: complete charge delocalization occurs in the case of $n = 1$, and substantial delocalization is retained with n up to 4 (Fc···Fc distance about 27 Å).[6,7]

The introduction of ferrocene carboxylate as the equatorial ligand is made possible by the facile synthesis of $Ru_2(DArF)_{4-n}(OAc)_n$ type compounds, which has been developed by Cotton et al.,[18,19] Jiménez-Aparicio et al.,[20,21] and us.[22−24] The DArF ligands employed include *N*,*N*′-di(*o*-methoxyphenyl)formamidinate), *N*,*N*′-diphenylformamidinate (DPhF), *N*,*N*′-di(*p*-anisyl)formamidinate (DpAniF), *N*,*N*′-di(3-methoxyphenyl)formamidinate (DmAniF), and *N*,*N*′-di(3,5-dichlorophenyl)formamidinate. Starting from $Ru_2(D(3,5\text{-}Cl_2Ph)F)_{4-n}(OAc)_nCl$ (n = 1 (**1a**), 2 (**2a**)), the ferrocene carboxylate containing derivatives $Ru_2(D(3,5\text{-}Cl_2Ph)F)_{4-n}(O_2CFc)_nCl$ (n = 1 (**3a**), 2 (**4a**), Scheme 1) were prepared, and the ET between two equatorial ferrocenyls in **4a** was explored in our prior communication.[9] In the present study, we expanded the synthesis and characterization to the analogous compounds based on DmAniF, $Ru_2(DmAniF)_{4-n}(O_2CFc)_nCl$ (n = 1 (**3b**), 2 (**4b**)), and explored the electronic structure of type **4** compounds with magnetic and DFT investigations.

Scheme 1. Synthesis of Compounds **3** and **4**

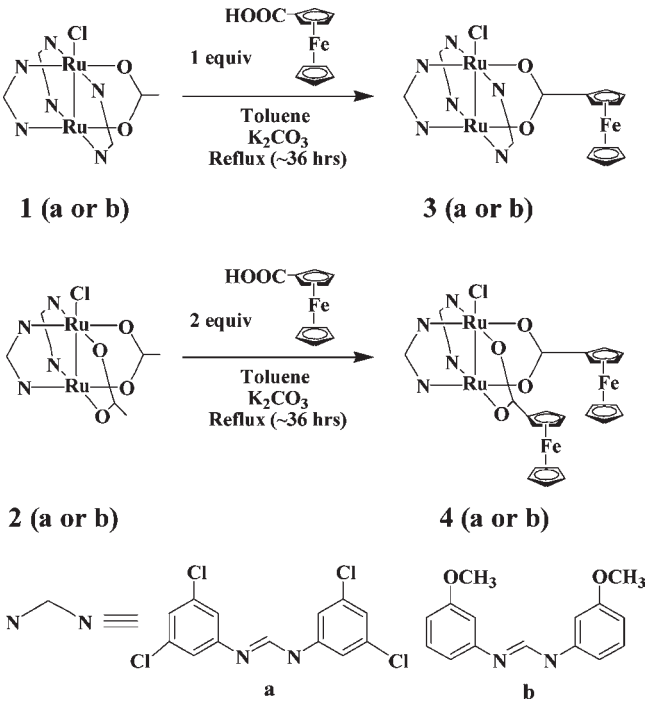

Results and Discussion

Syntheses of compounds **3** and **4** were achieved by refluxing the appropriate $Ru_2(DArF)_{4-n}(OAc)_nCl$ precursor with 1 and 2 equiv of FcCOOH, respectively, in a Schlenk flask outfit with a Soxhlet extractor containing K_2CO_3 as the scrubber for acetic acid, which was fashioned after that used by Doyle et al.[25] After the solvent removal, compounds **3a**, **3b**, and **4b** were purified by the recrystallization of crude product from THF/hexanes (1:9), CH_2Cl_2/hexanes (1:7), and CH_2Cl_2/hexanes (1:7), respectively. Compound **4a** was purified on a column using ethyl acetate/hexanes (v/v, 1:7 to 1:1).

Compounds **3** and **4** are paramagnetic with effective magnetic moments ranging from 3.59 to 4.00 Bohr magnetons

(10) Pauson, P. L. *J. Organomet. Chem.* **2001**, *637*, 3. Zanello, P. In *Ferrocenes: Homogeneous Catalysis, Organic Synthesis, Materials Science*; Togni, A., Hayashi, T., Eds.; VCH: New York, 1995. Barlow, S.; O'Hare, D. *Chem. Rev.* **1997**, *97*, 637. Geiger, W. E. *Organometallics* **2007**, *26*, 5738.
(11) Cowan, D. O.; Levanda, C.; Park, J.; Kaufman, F. *Acc. Chem. Res.* **1973**, *6*, 1.
(12) Lin, Y. C.; Chen, W. T.; Tai, J.; Su, D.; Huang, S. Y.; Lin, I.; Lin, J. L.; Lee, M. M.; Chiou, M. F.; Liu, Y. H.; Kwan, K. S.; Chen, Y. J.; Chen, H. Y. *Inorg. Chem.* **2009**, *48*, 1857. Liu, F.; Wu, X. H.; Xia, J. L.; Jin, S.; Yu, G. A.; Liu, S. H. *J. Organomet. Chem.* **2010**, *695*, 809. Diez, A.; Lalinde, E.; Moreno, M. T.; Sanchez, S. *Dalton Trans.* **2009**, 3434.
(13) Koridze, A. A.; Sheloumov, A. M.; Dolgushin, F. M.; Ezernitskaya, M. G.; Rosenberg, E.; Sharmin, A.; Ravera, M. *Organometallics* **2008**, *27*, 6163. Wei, Q. H.; Yin, G. Q.; Zhang, L. Y.; Chen, Z. N. *Organometallics* **2006**, *25*, 4941. Koshevoy, I. O.; Smirnova, E. S.; Domenech, A.; Karttunen, A. J.; Haukka, M.; Tunik, S. P.; Pakkanen, T. A. *Dalton Trans.* **2009**, 8392. de Biani, F. F.; Manca, G.; Marchetti, L.; Leoni, P.; Bruzzone, S.; Guidotti, C.; Atrei, A.; Albinati, A.; Rizzato, S. *Inorg. Chem.* **2009**, *48*, 10126.
(14) Auger, A.; Swarts, J. C. *Organometallics* **2007**, *26*, 102. Nemykin, V. N.; Rohde, G. T.; Barrett, C. D.; Hadt, R. G.; Bizzarri, C.; Galloni, P.; Floris, B.; Nowik, I.; Herber, R. H.; Marrani, A. G.; Zanoni, R.; Loim, N. M. *J. Am. Chem. Soc.* **2009**, *131*, 14969.
(15) Kaifer, A. E. *Eur. J. Inorg. Chem.* **2007**, 5015. Alvarez, J.; Ren, T.; Kaifer, A. E. *Organometallics* **2001**, *20*, 3543.
(16) Berry, J. F.; Cotton, F. A.; Murillo, C. A. *Organometallics* **2004**, *23*, 2503.
(17) Kuo, C. K.; Chang, J. C.; Yeh, C. Y.; Lee, G. H.; Wang, C. C.; Peng, S. M. *Dalton Trans.* **2005**, 3696.
(18) Angaridis, P.; Berry, J. F.; Cotton, F. A.; Murillo, C. A.; Wang, X. P. *J. Am. Chem. Soc.* **2003**, *125*, 10327. Angaridis, P.; Cotton, F. A.; Murillo, C. A.; Villagran, D.; Wang, X. P. *Inorg. Chem.* **2004**, *43*, 8290.
(19) Angaridis, P.; Berry, J. F.; Cotton, F. A.; Lei, P.; Lin, C.; Murillo, C. A.; Villagran, D. *Inorg. Chem. Commun.* **2004**, *7*, 9.
(20) Barral, M. C.; Herrero, S.; Jimenez-Aparicio, R.; Torres, M. R.; Urbanos, F. A. *Inorg. Chem. Commun.* **2004**, *7*, 42. Barral, M. C.; Gallo, T.; Herrero, S.; Jimenez-Aparicio, R.; Torres, M. R.; Urbanos, F. A. *Inorg. Chem.* **2006**, *45*, 3639. Barral, M. C.; Herrero, S.; Jimenez-Aparicio, R.; Priego, J. L.; Torres, M. R.; Urbanos, F. A. *J. Mol. Struct.* **2008**, *890*, 221. Barral, M. C.; Herrero, S.; Jimenez-Aparicio, R.; Torres, M. R.; Urbanos, F. A. *J. Organomet. Chem.* **2008**, *693*, 1597. Barral, M. C.; Casanova, D.; Herrero, S.; Jiménez-Aparicio, R.; Torres, M. R.; Urbanos, F. A. *Chem.—Eur. J.* **2010**, *16*, 6203. Añez, E.; Herrero, S.; Jiménez-Aparicio, R.; Priego, J. L.; Torres, M. R.; Urbanos, F. A. *Polyhedron* **2010**, *29*, 232.
(21) Barral, M. C.; Herrero, S.; Jimenez-Aparicio, R.; Torres, M. R.; Urbanos, F. A. *Angew. Chem., Int. Ed.* **2005**, *44*, 305. Barral, M. C.; Gallo, T.; Herrero, S.; Jimenez-Aparicio, R.; Torres, M. R.; Urbanos, F. A. *Chem.—Eur. J.* **2007**, *13*, 10088.
(22) Ren, T.; DeSilva, V.; Zou, G.; Lin, C.; Daniels, L. M.; Campana, C. F.; Alvarez, J. C. *Inorg. Chem. Commun.* **1999**, *2*, 301. Chen, W. Z.; Ren, T. *Organometallics* **2004**, *23*, 3766. Xu, G.-L.; Ren, T. *Inorg. Chem.* **2006**, *45*, 10449. Ren, T. *C. R. Chim.* **2008**, *11*, 684. Ren, T. *Chem. Rev.* **2008**, *108*, 4185. Fan, Y.; Liu, I. P. C.; Fanwick, P. E.; Ren, T. *Organometallics* **2009**, *28*, 3959.
(23) Chen, W. Z.; Ren, T. *Organometallics* **2005**, *24*, 2660.
(24) Chen, W. Z.; Ren, T. *Inorg. Chem.* **2006**, *45*, 8156.
(25) Doyle, M. P.; Bagheri, V.; Wandless, T. J.; Harn, N. K.; Brinker, D. A.; Eagle, C. T.; Loh, K. L. *J. Am. Chem. Soc.* **1990**, *112*, 1906. Doyle, M. P.; Winchester, W. R.; Hoorn, J. A. A.; Lynch, V.; Simonsen, S. H.; Ghosh, R. *J. Am. Chem. Soc.* **1993**, *115*, 9968. Zou, G.; Alvarez, J. C.; Ren, T. *J. Organomet. Chem.* **2000**, *596*, 152.

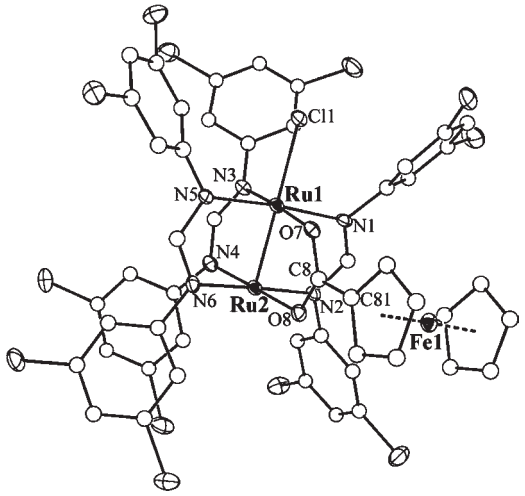

Figure 1. Structural plot of **3a**.

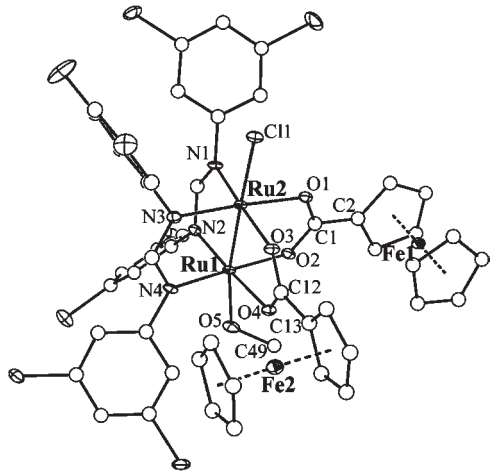

Figure 2. Structural plot of **4a**·MeOH.

(BM) at room temperature (298 K), which are close to the theoretical spin-only value of 3.87 μ_B. The effective magnetic moments of **3b** (3.59 μ_B) and **4b** (3.66 μ_B) are substantially lower than the expected spin-only value, which may be attributed to the existence of spin-admixture, i.e., equilibrium between $S = 3/2$ and $S = 1/2$ states, that has been advocated by Jiménez-Aparicio et al.[21] Because of the paramagnetism of **3** and **4**, important geometric features such as the ligand arrangement around the Ru_2 core cannot be established using NMR spectroscopy. Hence, molecular structures of compounds **3a** and **4a** were determined using single crystal X-ray diffraction, and the ORTEP plots of **3a** and **4a** are given in Figures 1 and 2, respectively. In addition to confirming the composition of compounds, Figure 2 also clearly shows the retention of *cis*-(2,2) ligand arrangement in **4a** and, hence, the absence of ligand scrambling during the carboxylate exchange reaction. The selected bond lengths and angles of **3a** and **4a** are provided in Table 1 along with the average bond lengths and angles of the parent compounds **1a** and **2a**.[24]

The metric parameters of the first coordination of Ru_2 in compounds **3a** and **4a** are very similar to those of parent compounds **1a** and **2a**. Specifically, the Ru−Ru bond lengths of **3a** (2.3141(8) Å) and **4a** (2.3141(8) Å) are slightly shortened from those of **1a** (2.3219(4) Å) and **2a** (2.3267(7) Å),[24] reflecting the better electron donating ability of ferrocenyl

Table 1. Selected Bond Lengths (Å) and Angles (deg) for Compounds **3a** and **4a** with the Average Bond Lengths and Angles of the Precursors **1a** and **2a**

3a		**4a**	
Ru1−Ru2	2.3141(8)	Ru1−Ru2	2.3169(5)
Ru1−Cl1	2.4078(18)	Ru1−O5	2.310(4)
Ru1−O7	2.075(4)	Ru1−O4	2.052(3)
Ru1−N1	2.092(6)	Ru1−O2	2.051(3)
Ru1−N3	2.075(6)	Ru1−N2	2.048(4)
Ru1−N5	2.097(6)	Ru1−N4	2.034(4)
Ru2−O8	2.042(5)	Ru2−Cl1	2.4628(13)
Ru2−N2	2.052(6)	Ru2−O3	2.065(3)
Ru2−N4	2.031(6)	Ru2−O1	2.071(3)
Ru2−N6	2.035(6)	Ru2−N1	2.052(4)
O7−C8	1.278(9)	Ru2−N3	2.048(4)
O8−C8	1.284(8)	O5−C49	1.484(13)
C8−C81	1.460(10)	O4−C12	1.268(7)
		O3−C12	1.276(6)
		C12−C13	1.471(7)
		O2−C1	1.266(6)
		O1−C1	1.271(6)
		C1−C2	1.460(7)
Ru2−Ru1−Cl1	176.85(5)	Ru1−O5−C49	120.4(5)
		Ru1−Ru2−Cl1	174.01(3)
		Ru2−Ru1−O5	168.82(11)

1a		**2a**	
Ru−Ru	2.3220(7)	Ru−Ru	2.3267(7)
Ru−N	2.064[6]	Ru−N	2.044[4]
Ru−O	2.079[5]	Ru−O	2.050[3]
Ru−Cl	2.405(2)	Ru−Cl	2.480(1)

carboxylate than that of acetate. The Ru−N and Ru−O distances in **3a** and **4a** are also comparable to those found for **1a** and **2a**. On close examination, one can notice that the Ru−N bond lengths on the Ru1 center in **3a** are significantly elongated compared to those on the Ru2 center, which is clearly caused by the attachment of an axial chloro ligand to Ru1. Less variation in the Ru−N bond lengths is noticed in **4a**, since the axial site of the second Ru center is occupied by a methanol solvent. Solvent coordination to the axial site has been a common feature for *cis*-(2,2) type compounds but is frequently absent in the (3,1) type compounds, reflecting the openness of the axial sites in the former. The presence of the second axial ligand apparently weakens the Ru−Cl bond, which is about 0.06 Å longer in the *cis*-(2,2) species (**2** and **4**) than that in the (3,1) species (**1** and **3**). Finally, the Fe···Fe distance in **4a** is 7.46 Å, a relatively short separation that may favor the through space Fc···Fc coupling.

Diruthenium paddlewheel complexes are known to have rich redox chemistry, often displaying several reversible and semireversible one-electron oxidation/reduction couples.[4] Compounds **3** and **4** are no exceptions. Cyclic voltammograms (CVs) of **3a** and **4a** were included in the earlier communication and are omitted here. Cyclic voltammograms (CVs) of **3b** and **4b** are shown in Figure 3 along with their parent compounds (**1b** and **2b**), and the assignment of the observed redox couples are given in Scheme 2.

The cathodic region of compound **3b** consists of an irreversible reduction (**B**), a reversible reduction (**C**), and an irreversible oxidation on the return sweep (**D**) that occurs at a far more positive potential than E_{pc}(**B**). It is clear from Figure 3 that the cathodic behavior of **3b** is nearly identical to that of **1b** and, hence, is independent of the presence of a ferrocenyl group as one might expect. The appearance of two irreversible peaks is related to the dissociation of the axial chloro ligand in an ECE mechanism first proposed for a Ru_2 species by Kadish and co-workers.[26] The initial reduction of

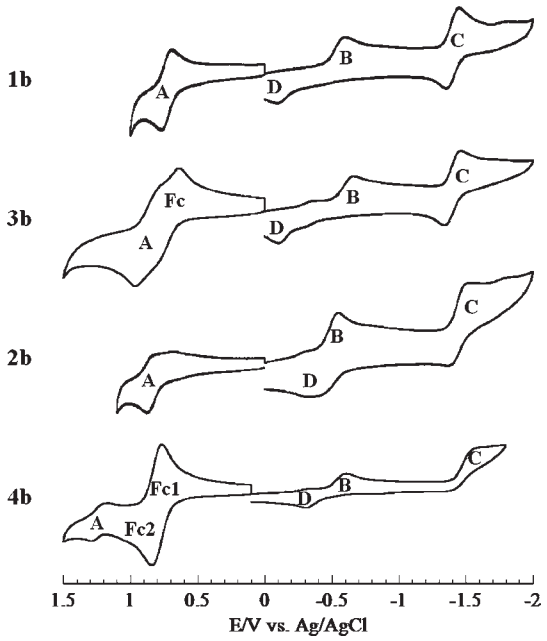

Figure 3. CVs of $Ru_2(DmAniF)_3(OAc)Cl$ (**1b**), $Ru_2(DmAniF)_2(OAc)_2Cl$ (**2b**), $Ru_2(DmAniF)_3(O_2CFc)Cl$ (**3b**), and $Ru_2(DmAniF)_2(O_2CFc)_2Cl$ (**4b**). Results recorded in a 0.20 M THF solution of Bu_4NPF_6 at a scan rate of 0.10 V/s.

Scheme 2. Assignments of the Ru_2-Based Redox Couples

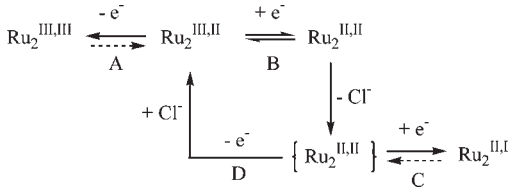

$Ru_2^{III,II}$ to $Ru_2^{II,II}$ (**B**) significantly enhances the electron richness at the Ru_2 core, which triggers the complete dissociation of Cl^-. The second couple (**C**) is related to the Ru_2 species that is free of axial Cl^- and hence quite reversible. The peak designated **D** corresponds to the reoxidation of the chloro-less species and thus appears at a more positive potential than E_{pc}(**B**) since chloro is a moderate electron donor.

The anodic region of the CV of **3b** consists of two closely spaced quasi-reversible $1e^-$ couples—one from the Ru_2 center and the other from the ferrocenyl group. On the basis of both the position of the Ru_2-based couple (**A**) in **1b** and the assignment of anodic couples in **3a**, the first (less anodic) couple is assigned to Fc and the second to Ru_2. The position of **A** in **3b** is significantly shifted to a more cathodic direction than that of **3a**, which is attributed to the strong electron withdrawing nature of the 3,5-Cl_2 substituent.[27] Additionally, the oxidation couple **A** is slightly more positive in **3b** than it is in **1b** as a result of positive charge gained upon the oxidation of the ferrocene center.

As with **1b** and **3b**, similarities in the cathodic range of **2b** and **4b** are also apparent. The irreversible couples **B** and **D** arise as a result of the fast dissociation of the axial Cl^- similar to the (3,1) species **1** and **3**. The couple **C** becomes irreversible

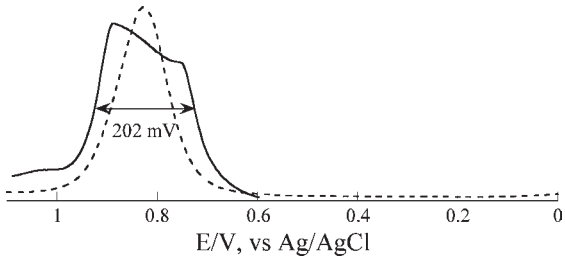

Figure 4. DPVs of the ferrocenyl oxidation region measured for **4b** under both the normal conditions (dash) and conditions according to Richardson−Taube (solid).

in compounds **2** and **4**, indicating that the *cis*-(2,2) type compounds are highly susceptible to degradation upon reduction by dissociating both chloro and carboxylate ligands. The anodic region of the CV of compound **4b** is quite distinctive from that of **2b**: there is a reversible pseudo-two-electron couple that is attributed to both ferrocenyls and a quasi-reversible couple (**A**) to the Ru_2 center. Compared with **2b**, the **A** couple in **4b** is much more positive—likely due to the presence of two ferrocene moieties in the structure of the compound. Unlike **4a**, the stepwise nature of ferrocene oxidations in **4b** is not obvious from either CV (Figure 3) or the DPV recorded under the typical conditions (Figure 4). To estimate the separation of two $1e^-$ couples, we invoked the model developed by Richardson and Taube,[28] which was successfully utilized in resolving similar overlapping Fc oxidations.[16,29] Specifically, the DPV of **4b** was measured sequentially in increments of 10 mV, going from a pulse amplitude of 50 mV down to 10 mV, yielding a width of 202 mV (Figure 4) that corresponds to a $\Delta E_{1/2}$ of *ca.* 110 mV according to the Richardson−Taube model.[28] Similar analysis of the DPV of **4a** (see Figure S1 of the Supporting Information) yielded a $\Delta E_{1/2}$ of *ca.* 110 mV.

Previously, $Ru_2(O_2CFc)_4Cl$ and related compounds were prepared and characterized by Aquino and co-workers, and equatorial Fc···Fc interactions were inferred from the electrochemical studies.[30] While the stepwise Fc oxidations observed in both **4a** and **4b** constituted circumstantial evidence for equatorial coupling, ascertaining the nature of the $[Fc\cdots Fc]^+$ mixed valency in **4** will provide unequivocal proof of the coupling. In order to further study the spectroscopic and magnetic properties of the mixed species, cations $[\mathbf{4}]^+$ were generated by treating **4** with $AgBF_4$ in slight excess in THF and isolated as the $[\mathbf{4}]BF_4$ salt in the case of **4a**.[31] Metallic silver was recovered in quantitative yield in a large scale preparation of $[\mathbf{4a}]BF_4$.

The vis−NIR spectra of compounds **4b** and $[\mathbf{4b}]BF_4$ are shown in Figure 5, while those of **4a** and $[\mathbf{4a}]BF_4$ can be found in the previous communication.[9] Spectra of the neutral compounds **4** both feature intense absorptions (at 21 500 and 17 500 cm^{-1} for **4b**) in the visible region that are likely associated with ligand-to-metal charge transfer at the Ru_2 core. In the spectrum of $[\mathbf{4b}]BF_4$, the peak at 21 500 cm^{-1} is

(26) Bear, J. L.; Han, B.; Huang, S.; Kadish, K. M. *Inorg. Chem.* **1996**, *35*, 3012.
(27) Ren, T. *Coord. Chem. Rev.* **1998**, *175*, 43. Lin, C.; Ren, T.; Valente, E. J.; Zubkowski, J. D.; Smith, E. T. *Chem. Lett.* **1997**, 753.
(28) Richardson, D. E.; Taube, H. *Inorg. Chem.* **1981**, *20*, 1278.
(29) Xu, G.-L.; Xi, B.; Updegraff, J. B.; Protasiewicz, J. D.; Ren, T. *Organometallics* **2006**, *25*, 5213.
(30) Cooke, M. W.; Murphy, C. A.; Cameron, T. S.; Swarts, J. C.; Aquino, M. A. S. *Inorg. Chem. Commun.* **2000**, *3*, 721. Cooke, M. W.; Cameron, T. S.; Robertson, K. N.; Swarts, J. C.; Aquino, M. A. S. *Organometallics* **2002**, *21*, 5962.
(31) Connelly, N. G.; Geiger, W. E. *Chem. Rev.* **1996**, *96*, 877.

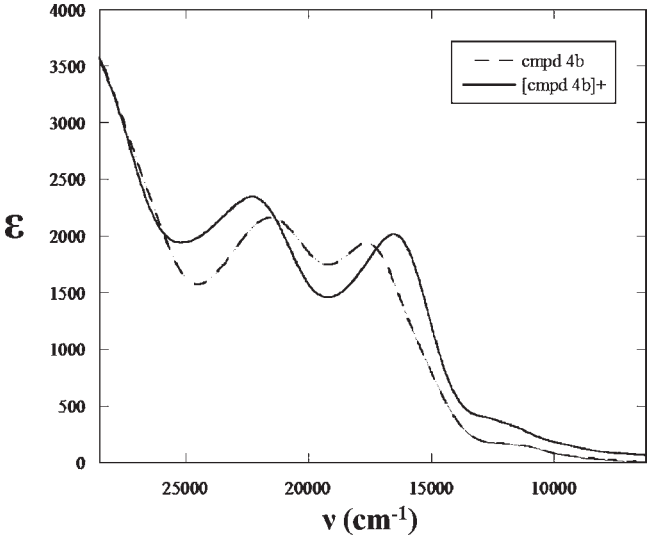

Figure 5. Vis−NIR spectra of compounds **4b** and [**4b**]$^+$ recorded in THF.

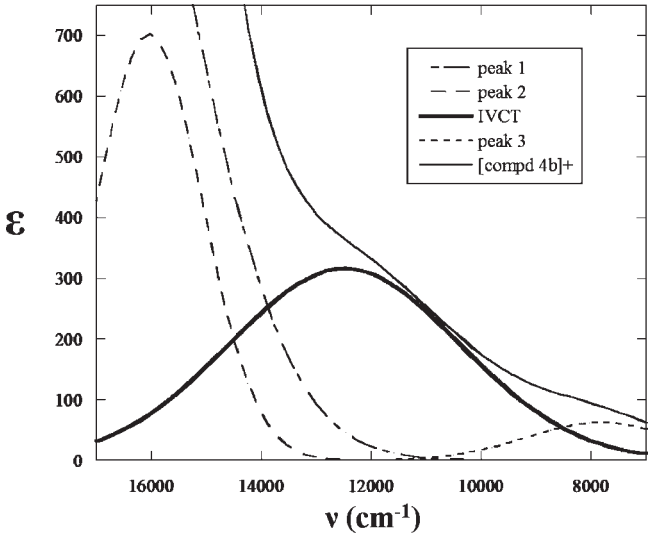

Figure 6. Gaussian deconvolution of the compound [**4b**]BF_4 vis−NIR spectrum recorded in THF.

blue-shifted, while the peak at 17 500 cm^{-1} is red-shifted. Similar spectral changes were also observed for [**4a**]BF_4. However, the most appealing feature is the appearance of a broad shoulder in the region between 15 000 and 10 000 cm^{-1}, where the intervalence charge transfer transition is expected for $[Fc\cdots Fc]^+$ species.[11] Gaussian deconvolution of the vis−NIR region of [**4b**]BF_4 returns a broad peak that is assigned as the IVCT band (Figure 6). The ν_{max} and $\Delta\nu_{1/2}$ of the IVCT band were estimated to be 12 500 cm^{-1} and 5000 cm^{-1}, respectively, for **4b**, and 13 100 and 5500 cm^{-1} for **4a**. The calculated half widths according to the Hush model[32] are 5501 and 5370 cm^{-1} for [**4a**]$^+$ and [**4b**]$^+$, respectively, which support a Robin−Day class II mixed valent species designation for [**4**]$^+$.[32,33] The vis−NIR spectrum of [**4a**]$^+$ (see Figure S2 of the Supporting Information) was also recorded in CH_3CN ($\varepsilon_r = 37.5$), which is far more polar than THF ($\varepsilon_r = 7.5$), where the appearance of the broad shoulder attributed to the IVCT at *ca.* 800 nm remains essentially unchanged. The independence of the IVCT band on solvent polarity indicates that the electron transfer between two Fc centers occurs likely through the covalent bonds instead of space.

The room temperature effective magnetic moments of compounds **3** and **4** range between 3.4 and 3.8 Bohr magnetons, which are consistent with an $S = 3/2$ ground state similar to those of homoleptic compounds $Ru_2(O_2CR)_4Cl$ and $Ru_2(DArF)_4Cl$.[34,35] The magnetism of the mixed valence species [**4**]$^+$ offers an intriguing scenario because of the coexistence of $S = 3/2$ (Ru_2) and $S = 1/2$ (Fe^{III} of Fc^+) centers. To unravel the magnetic interaction in [**4**]$^+$, the magnetic susceptibilities of both [**4a**]BF_4 and its parent compound **4a** were measured over the temperature window of 2−300 K, and data plots are shown in Figure 7. The temperature dependence of χT of **4a** can be easily modeled using the zero-field splitting (ZFS) model with mean-field correction described in the following equations:[36]

$$\chi_{||} = \frac{Ng^2\beta^2}{kT}\,\frac{1+9\,e^{-2x}}{4(1+e^{-2x})} \tag{1}$$

$$\chi_{\perp} = \frac{Ng^2\beta^2}{kT}\,\frac{4+\frac{3}{x}(1-e^{-2x})}{4(1+e^{-2x})} \tag{2}$$

$$\chi = (\chi_{||} + 2\chi_{\perp})/3 \tag{3}$$

$$\chi_M = \frac{\chi}{1-(2zj'/Ng^2\beta^2)\chi} \tag{4}$$

where x is $D/(kT)$ and D is the magnitude of the ZFS. The best fit yielded $D = 77.3(9)$ cm^{-1}, $g = 1.903(1)$, and $zj = -0.039(3)$ cm^{-1} with $R = \Sigma[(\chi_M T)_{calc} - (\chi_M T)_{obs}]^2/\Sigma(\chi_M T)_{obs}{}^2 = 5 \times 10^{-5}$. The D value is comparable to those determined for $Ru_2(DAniF)_3(OAc)Cl$ (70 cm^{-1}, DAniF = di(*p*-methoxyphenyl)formamidinate)[19] and $Ru_2(D(3,5\text{-}Cl_2\text{-}Ph)F)_4Cl$ (79 cm^{-1}).[35] The mean-field correction constant zj' is very small and negligible, indicating that the intermolecular magnetic interaction in **4a** hardly exists.

The temperature dependence of χT of [**4a**]BF_4 can be modeled using a method similar to that used for **4a**, where the paramagnetic contribution of Fc^+ is taken into account and zj' represents the *intramolecular* magnetic coupling between Ru_2 and Fc^+ because of the negligible intermolecular magnetic interaction. Thus, eq 3 can be modified as below:

$$\chi = (\chi_{||} + 2\chi_{\perp})/3 + \frac{Ng^2\mu_B^2}{3kT}\,S_{Fc^+}(S_{Fc^+}+1) \tag{3'}$$

The fitting led to $D = 77(1)$ cm^{-1}, $g = 2.006(2)$, $zj' = -0.76(1)$ cm^{-1}, and $R = 1.5 \times 10^{-4}$. The ZFS constant is in excellent

(32) Hush, N. *Prog. Inorg. Chem.* **1967**, *8*, 391.
(33) Robin, M.; Day, P. *Adv. Inorg. Chem. Radiochem.* **1967**, *10*, 1396.
(34) Angaridis, P. In *Multiple Bonds between Metal Atoms*; Cotton, F. A., Murillo, C. A., Walton, R. A., Eds.; Springer Science and Business Media, Inc.: New York, 2005.
(35) Chen, W.-Z.; Cotton, F. A.; Dalal, N. S.; Murillo, C. A.; Ramsey, C. M.; Ren, T.; Wang, X.; Wernsdorfer, W. *J. Am. Chem. Soc.* **2005**, *127*, 12691.
(36) O'Connor, C. J. *Prog. Inorg. Chem.* **1982**, *29*, 203.

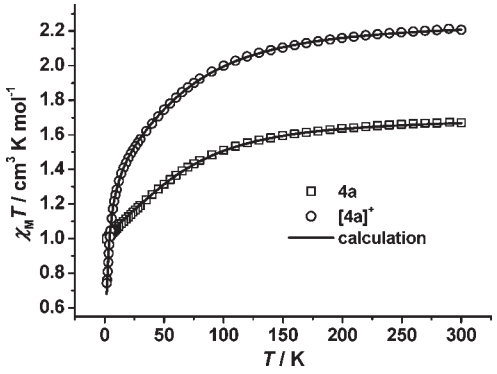

Figure 7. Temperature dependences of magnetic properties in the form of $\chi_M T$ for **4a** and [**4a**]BF_4 (□ and ○) and the theoretical fit according to the ZFS model (solid lines).

agreement with that of **4a**, and the relative small value of zj' is consistent with a weak antiferromagnetic coupling between Ru_2 and Fc^+.

It should be noted that the voltammetric and magnetic data appear to be at odds with regard to the nature of the highest occupied MOs in compounds **4**. The magnetic data for **4a** and other Ru_2(II,III)'s are consistent with a $\pi^*(Ru_2)^2\delta^*(Ru_2)^1$ configuration and hence place the Ru_2 based orbitals atop the occupied MOs. The voltammetry and IVCT analysis indicate that the first electron removed upon oxidation is from a MO localized on the Fc centers. This behavior perhaps reflects the energy levels of $\delta^*(Ru_2)$, $\pi^*(Ru_2)$, and some of the Fc localized orbitals, being very close in energy, which results in an apparent violation of Koopmans' theorem.[37] Qualitatively, the ionization energy of $\delta^*(Ru_2)$ is $-E(\delta^*)$, while that of Fc is $-E(Fc) - P$, where P is the pairing energy since the ferrocene-based orbitals are filled. Hence, the energetic difference in ionizing ferrocene and ionizing the Ru_2 core is $(-E(Fc) - P) - (-E(\delta^*)) = -P + (E(\delta^*) - E(Fc)) = -P + \Delta$. Since the computed Δ (0.10 eV) is much smaller than the pairing energy,[38] ionization of ferrocene is favored.

Molecular orbital calculations (DFT) for the model compounds of **3** and **4** were obtained using the BP86, BPW91, and B3LYP type basis sets. While these calculations are self-consistent in terms of the nature of frontier orbitals, they did not yield the configuration that is expected from the voltammetric and magnetic studies. Hence, the details are provided as part of the Supporting Information. The calculations did reveal the absence of a molecular orbital that contains significant contributions from the Ru_2, Fe centers, and Cp rings *simultaneously* in compound **4**. Hence, the weak delocalization in [**4**]$^+$ is likely caused by the lack of a proper superexchange pathway between two ferrocene centers, which forces the delocalized electron (or hole) to hop from site to site.

Conclusions

$Ru_2(DArF)_{4-n}(O_2CFc)_nCl$ (n = 1, **3**; 2, **4**) was prepared and characterized. The voltammetric data of bis-ferrocene compounds **4** and the IVCT characteristics of the corresponding cations [**4**]BF_4 indicate that two equatorial ferrocenes are weakly coupled. Poor π orbital interactions between the Ru_2 core and $FcCO_2^-$ and the lack of a direct superexchange pathway are probably responsible for the weak coupling.

Experimental Section

Ferrocene carboxylic acid was purchased from Alfa Aesar, silver nitrate from Mallinckrodt Baker, and silver tetrafluoroborate from Strem Chemicals. $Ru_2(D(3,5\text{-}Cl_2Ph)F)_3(OAc)Cl$ (**1a**), $Ru_2(DmAniF)_3(OAc)Cl$ (**1b**), *cis*-$Ru_2(D(3,5\text{-}Cl_2Ph)F)_2(OAc)_2Cl$ (**2a**), and *cis*-$Ru_2(DmAniF)_2(OAc)_2Cl$ (**2b**) were prepared as previously described.[23,24] Vis−NIR spectra in THF were obtained with a JASCO V-670 spectrophotometer. Room temperature magnetic susceptibilities of compounds **3** and **4** were measured using a Johnson Matthey Mark-I Magnetic Susceptibility Balance. Temperature dependent magnetic susceptibility data for compounds **4a** and [**4a**]BF_4 were obtained with the use of a Quantum Design MPMS-XL7 SQUID magnetometer at a temperature range of 1.8−300 K under an applied field of 2 kOe. Elemental analysis was performed by Atlantic Microlab, Norcross, Georgia. Cyclic voltammograms were recorded in a 0.2 M $(n\text{-}Bu)_4NPF_6$ solution (THF, N_2-degassed) on a CHI620A voltammetric analyzer with a glassy carbon working electrode (diameter = 2 mm), a Pt-wire auxiliary electrode, and a Ag/AgCl reference electrode. The concentration of diruthenium species is always 1.0 mM. The ferrocenium/ferrocene couple was observed at 0.58 V vs Ag/AgCl under the experimental conditions.

Preparation of $Ru_2(D(3,5\text{-}Cl_2Ph)F)_3(O_2CFc)Cl$ (3a). A 100 mL round bottomed flask was charged with **1a** (0.558 g, 0.429 mmol), ferrocene carboxylic acid (0.105 g, 0.456 mmol), and toluene (80 mL). The flask was mounted with a Soxhlet extractor containing a thimble that is charged with potassium carbonate covered by sand, which served as the scrubber for acetic acid. The solution was allowed to reflux via a sand-filled heating mantle, and the progress was monitored with TLC (EtOAc/hexanes, 1:7, v/v), which indicated the complete consumption of **1a** after about 36 h. After the solvent removal on a rotavap, the residue was recrystallized from THF/hexanes (1:9) to afford 0.241 g of purple crystalline materials (43.0% based on Ru_2). Data for **3a** are as follows. ESI-MS (m/z, based on ^{101}Ru): 1430 $[M - Cl]^+$. R_f = 0.37 (EtOAc/hexanes, 1:7). Anal. Found (Calcd) for $C_{54}H_{38}Cl_{13}N_6O_3Ru_2Fe$ (**3a**·1.0THF): C, 42.1 (42.2); H, 2.38 (2.49); N, 5.48 (5.47). Vis, λ_{max} (nm, ε (M^{-1} cm^{-1})): 517 (6400). χ_{mol} (corrected) = 6.43×10^{-3} emu. $\mu_{eff} = 3.92\,\mu_B$. Cyclic voltammogram $E_{1/2}$/V, ΔE_p/V, $i_{backward}/i_{forward}$: **A**, 1.160, 0.040, 0.82; **B**, −0.239, 0.020, 0.700; E_{pc}(**C**), −1.470; **D**, −1.015, 0.044, 0.64.

Preparation of $Ru_2(DmAniF)_3(O_2CFc)Cl$ (3b). Compound **3b** was prepared from the reaction between **1b** (0.442 g, 0.416 mmol) and ferrocene carboxylic acid (0.111 g, 0.440 mmol) under the same conditions as those of **3a**, and the recrystallization of the crude product from CH_2Cl_2/hexanes (1:7) afforded 0.340 g of purple crystalline materials (76.9% based on Ru_2). Data for **3b** are as follows. ESI-MS (m/z, based on ^{101}Ru): 1198 $[M-Cl]^+$. R_f = 0.70 (acetone/CH_2Cl_2, 1:2). Anal. Found (Calcd) for $C_{59.5}H_{61}ClN_6O_8Ru_2Fe$ (**3b**·$1H_2O$·$0.5C_7H_8$): C, 55.1 (55.1); H, 4.74 (4.66); N, 6.48 (6.48). Vis, λ_{max} (nm, ε (M^{-1} cm^{-1})): 528 (18 900). χ_{mol} (corrected) = 5.40×10^{-3} emu. μ_{eff} = 3.59 μ_B. Cyclic voltammogram $E_{1/2}$/V, ΔE_p/V, $i_{backward}/i_{forward}$: **A**, 0.869, 0.032, 0.97; E_{pc}(**B**), −0.614; **C**, −1.393, 0.049, 0.62; E_{pc}(**D**), −0.111.

Preparation of *cis*-$Ru_2(D(3,5\text{-}Cl_2Ph)F)_2(O_2CFc)_2Cl$ (4a). Compound **2a** (0.222 g, 0.217 mmol) and ferrocene carboxylic acid (0.102 g, 0.443 mmol) were refluxed in the same setup as that of **3a** for 36 h. The crude reaction product was purified on a silica gel column using EtOAc/hexanes (v/v, 1:7 to 1:1) to afford

(37) Szabo, A. *Modern Quantum Chemistry: Introduction to Advanced Electronic Structure Theory*; McGraw-Hill: New York, 1989.

(38) A precise value of pairing energy for ferrocene cannot be found in the literature; the 3d−3d pairing energy for Fe atom was estimated to be 0.173 au (4.71 eV) in: Kelly, H.; Ron, A. *Phys. Rev. A* **1971**, *4*, 11.

0.124 g of deep red crystals (55.9% based on Ru_2). Data for **4a** are as follows. ESI-MS (m/z, based on ^{101}Ru): 1327 $[M - Cl]^+$. R_f = 0.55 (EtOAc/hexanes, 1:2). Anal. Found (Calcd) for $C_{53}H_{47}Cl_9N_4O_8Ru_2Fe_2$ (**4a**·0.5hexane·4H_2O): C, 43.0(42.4); H, 3.75(3.16); N, 3.65(3.73). Vis, λ_{max} (nm, ε (M^{-1} cm^{-1})): 524 (4100). χ_{mol} (corrected) = 6.72×10^{-3} emu. $\mu_{eff} = 4.00\,\mu_B$. Cyclic voltammogram $E_{1/2}$/V, ΔE_p/V, $i_{backward}/i_{forward}$: E_{pa}(**A**), 1.350; **B**, −0.334, 0.067, 0.53; E_{pc}(**C**), −1.361.

Preparation of *cis*-Ru_2(DmAniF)$_2$(O_2CFc)$_2$Cl (4b). Compound **2b** (0.102 g, 0.118 mmol) and ferrocene carboxylic acid (0.056 g, 0.242 mmol) were refluxed for 36 h in the same setup as that for compound **3a**. After the solvent removal, the residue was recrystallized from CH_2Cl_2/hexanes (1:7) to afford 0.088 g of green crystalline materials (86% based on Ru_2). Data for **4b** are as follows. ESI-MS (m/z, based on ^{101}Ru): 1172 $[M - Cl]^+$. R_f = 0.32 (acetone/CH_2Cl_2, 1:2). Anal. Found (Calcd) for $C_{55.5}H_{56}ClN_4O_8Ru_2Fe_2$ (**4b**·1H_2O·0.5C_7H_8): C, 52.4 (52.5); H, 4.44 (4.28); N, 4.40 (4.41). Vis, λ_{max} (nm, ε (M^{-1} cm^{-1})): 465 (21 500). χ_{mol} (corrected) = 5.61×10^{-3} emu. $\mu_{eff} = 3.66\,\mu_B$. Cyclic voltammogram $E_{1/2}$/V, ΔE_p/V, $i_{backward}/i_{forward}$: **A**, 1.229, 0.049, 0.99; E_{pc}(**B**), −0.606; E_{pc}(**C**), −1.600; E_{pc}(**D**), −0.306.

Oxidation of *cis*-Ru_2(*D*Ar*F*)$_2$(O_2CFc)$_2$Cl (4a and 4b). Compound **4a** (0.200 g) and $AgBF_4$ (1.3 equiv, 0.036 g) were stirred in 20 mL of dry THF under N_2 for 2 h. The reaction mixture was filtered through a fine glass frit to yield a dark green solution. The dark residue collected on the frit (0.0156 g) could not be dissolved in concentrated NH_3(aq), indicating that it was Ag(s) (theoretical yield based on **4a**: 0.0159 g) instead of AgCl(s). The filtrate was subsequently recrystallized from CH_2Cl_2/hexanes (1:9) to yield 0.193 g of [**4a**]BF_4 (91% based on **4a**). Compound **4b** (0.062 g) was similarly oxidized by the addition of $AgBF_4$ (0.012 g; 1.2 equiv) in 10 mL of THF and used directly for spectral analysis.

Structure Determination. Single crystals of compounds **3a** and **4a** were grown from hexanes/CH_2Cl_2 and CH_3OH/*o*-dichlorobenzene solutions, respectively. X-ray diffraction data were collected on a Rigaku Rapid II image plate diffractometer using Cu Kα radiation (λ = 1.54184 Å) at 150 K, and the structures were solved using the structure solution program PATTY in DIRDIF99[39] and refined using SHELX-07.[40] Crystal data for **3a**·2CH_2Cl_2: $C_{52}H_{34}Cl_{17}FeN_6O_2Ru_2$, fw = 1635.58, triclinic, $P\bar{1}$, a = 11.0193(7), b = 13.281(1), c = 23.350(1) Å, α = 92.43(7), β = 101.54(5), γ = 114.35(5)°, V = 3020.1(4) Å^3, Z = 2, D_{calcd} = 1.798 g cm^{-3}, R1 = 0.063, wR2 = 0.167. Crystal data for (**4a**·CH_3OH)·CH_3OH: $C_{50}H_{40}Cl_9Fe_2N_4O_6Ru_2$, fw = 1635.58, monoclinic, $P2_1/c$, a = 11.8533(4), b = 20.6367(6), c = 21.9307(5) Å, β = 90.15(2)°, V = 5364.5(3) Å^3, Z = 4, D_{cacl} = 1.765 g cm^{-3}, R1 = 0.051, wR2 = 0.138.

Acknowledgment. This work is supported in part by Purdue University, the National Science Foundation (grant CHE 0715404 to T.R.), and the National Natural Science Foundation of China (20725104, 20771057, 20531040 to Y.S.).

Supporting Information Available: Vis−NIR spectrum of [**4a**]BF_4 in CH_3CN. Details of DFT calculations of model compounds **4′** and **2′**. X-ray crystallographic files in CIF format for **3a** and **4a**. This material is available free of charge via the Internet at http://pubs.acs.org.

(39) Beurskens, P. T.; Beurskens, G.; deGelder, R.; Garcia-Granda, S.; Gould, R. O.; Smits, J. M. M. *The DIRDIF2008 Program System*; Crystallography Laboratory, University of Nijmegen: Nijmegen, The Netherlands, 2008.
(40) Sheldrick, G. M. *Acta Crystallogr., Sect. A* **2008**, *64*, 112.